Title

Role of a Class Dhc1b Dynein in Retrograde Transport of Ift Motors and Ift Raft Particles along Cilia, but Not Dendrites, in Chemosensory Neurons of Living Caenorhabditis elegans

Journal

Journal of Cell Biology, 147(3)

ISSN

0021-9525

Authors

Signor, Dawn

Wedaman, Karen P

Orozco, Jose T

et al.

Publication Date

1999-11-01

DOI

10.1083/jcb.147.3.519

Peer reviewed

Role of a Class DHC1b Dynein in Retrograde Transport of IFT Motors and IFT Raft Particles Along Cilia, but Not Dendrites, in Chemosensory Neurons of Living *Caenorhabditis elegans*

Dawn Signor,* Karen P. Wedaman,* Jose T. Orozco,* Noelle D. Dwyer,‡ Cornelia I. Bargmann,‡ Lesilee S. Rose,* and Jonathan M. Scholey*

*Section of Molecular and Cellular Biology, University of California Davis, Davis, California 95616; and ‡Department of Anatomy, Howard Hughes Medical Institute, University of California, San Francisco, San Francisco, California 94143

Abstract. The heterotrimeric motor protein, kinesin-II, and its presumptive cargo, can be observed moving anterogradely at 0.7 μm/s by intraflagellar transport (IFT) within sensory cilia of chemosensory neurons of living *Caenorhabditis elegans*, using a fluorescence microscope–based transport assay (Orozco, J.T., K.P. Wedaman, D. Signor, H. Brown, L. Rose, and J.M. Scholey. 1999. *Nature.* 398:674). Here, we report that kinesin-II, and two of its presumptive cargo molecules, OSM-1 and OSM-6, all move at ~1.1 μm/s in the retrograde direction along cilia and dendrites, which is consistent with the hypothesis that these proteins are retrieved from the distal endings of the cilia by a retrograde transport pathway that moves them along cilia and then dendrites, back to the neuronal cell body. To test the hypothesis that the minus end–directed microtubule motor protein, cytoplasmic dynein, drives this retrograde transport pathway, we visualized movement of kinesin-II and its cargo along dendrites and cilia in a *che-3* cytoplasmic dynein mutant background, and observed an inhibition of retrograde transport in cilia but not in dendrites. In contrast, anterograde IFT proceeds normally in *che-3* mutants. Thus, we propose that the class DHC1b cytoplasmic dynein, CHE-3, is specifically responsible for the retrograde transport of the anterograde motor, kinesin-II, and its cargo within sensory cilia, but not within dendrites.

Key words: dynein • kinesin • intraflagellar transport • *Caenorhabditis elegans* • neuron transport

INTRACELLULAR transport systems that utilize microtubules and microtubule-based motor proteins play important roles in many basic activities of eukaryotic cells including, for example, vesicle transport and ciliogenesis (Bi et al., 1997; Morris and Scholey, 1997). The action of such microtubule-based transport systems is very obvious within the cytoplasmic extensions that occur on certain cells, such as neuronal axons and dendrites, as well as motile and sensory cilia. Axons, dendrites, and cilia all deploy microtubule-based motor proteins to transport molecules from their site of synthesis in the cell body to the distal tip of the process (Rosenbaum et al., 1999; Goldstein and Yang, in press).

Microtubule-based transport in neuronal extensions has been studied extensively and, consequently, it is now well-established that numerous members of the kinesin and dynein superfamilies contribute to fast axonal transport (Hirokawa, 1998; Goldstein and Yang, in press). For example, members of the kinesin superfamily (Vale and Fletterick, 1997; Green and Henikoff, 1996) that move toward the plus ends of microtubule tracks drive the anterograde transport of vesicles from the neuronal cell body to the synaptic termini, where their protein and lipid components are needed. Movement of similar molecules in the reverse direction occurs during retrograde fast axonal transport, which is thought to depend on the action of minus end–directed kinesins as well as cytoplasmic dynein (Holzbaur and Vallee, 1994). Intradendritic transport is less well characterized, but it is also thought that some members of the kinesin superfamily serve to transport their cargo along dendritic processes (Saito et al., 1997; Marszalek et al., 1999a).

Intraflagellar transport (IFT)[1] is a more recently de-

Address correspondence to Dr. Jonathan M. Scholey, Section of Molecular and Cellular Biology, 1 Shields Avenue, University of California, Davis, Davis, CA 95616. Tel.: (530) 752-2271. Fax: (530) 752-7522. E-mail: jmscholey@ucdavis.edu

1. *Abbreviations used in this paper:* DHC, dynein heavy chain; IFT, intraflagellar transport; KAP, kinesin-II accessory polypeptide; ORF, open reading frame.

scribed phenomenon in which proteins that are required for the formation and maintenance of cilia or flagella are transported in the form of large protein complexes, IFT rafts, from their site of synthesis in the cell body, along axonemal microtubules just beneath the plasma membrane, to the distal tip of the axoneme (Johnson and Rosenbaum, 1992; Rosenbaum et al., 1999; Kozminski et al., 1993, 1995; Piperno and Mead, 1997; Cole et al., 1998; Orozco et al., 1999). IFT is required for the assembly and maintenance of motile cilia and flagella (Kozminski et al., 1995; Morris and Scholey, 1997), sensory cilia (Perkins et al., 1986; Tabish et al., 1995), and nodal cilia (Nonaka et al., 1998; Marszalek et al., 1999b).

Kinesin and dynein motors drive the bidirectional transport of IFT rafts between the base and the distal tip of motile and sensory cilia and flagella (Rosenbaum et al., 1999). For example, the anterograde movement of IFT rafts is driven by heterotrimeric kinesin-II (Cole et al., 1993; Wedaman et al., 1996; Scholey, 1996) as a mutant allele of the *fla-10* gene, which encodes a subunit of kinesin-II (Walther et al., 1994), gives rise to a cessation of raft movement and subsequent resorption of flagella in *Chlamydomonas* (Kozminski et al., 1995; Cole et al., 1998). Moreover, the anterograde transport of kinesin-II and its presumptive cargo in *Caenorhabditis elegans* sensory cilia now has been directly visualized by time-lapse fluorescent microscopy (Orozco et al., 1999). Conversely, the retrograde transport of IFT rafts in *Chlamydomonas* is facilitated by cytoplasmic dynein, as both a dynein heavy chain (DHC) mutant (*dhc1b*) and a dynein light chain mutant (*fla-14*) exhibit shortened and paralyzed flagella and an accumulation of raft particles at the flagellar tip (Pazour et al., 1998, 1999; Porter et al., 1999). This accumulation of raft particles is apparently due to the normal and continuous delivery of rafts in the anterograde direction (toward the flagellar tip) but defective retrieval.

The DHC1b class of dyneins is placed phylogenetically between the axonemal and cytoplasmic classes of DHC. DHC1b is a divergent dynein isotype that is present in both ciliated and nonciliated cells, and may play roles in Golgi organization as well as intraflagellar transport (Gibbons et al., 1994; Criswell et al., 1996; Pazour et al., 1999; Porter et al., 1999; Vaisberg et al., 1996). The *Chlamydomonas* DHC1b polypeptide shares high homology with the *C. elegans* CHE-3 protein (Pazour et al., 1999; Wicks, S., C. deVries, H. Van Luenen, and R. Plasterk, manuscript submitted for publication; Grant, W., personal communication), suggesting that CHE-3 is the *C. elegans* orthologue of DHC1b, and may play roles in retrograde traffic in nematodes.

Elegant biochemical and genetic studies done in *Chlamydomonas* have provided evidence that the basic subunit of IFT rafts is a 16S multiprotein complex containing at least 16 polypeptides, two of which share sequence homology with the OSM-1 and OSM-6 proteins that are required for sensory ciliary function in *C. elegans* (Piperno and Mead, 1997; Cole et al., 1998; Piperno et al., 1998). Sensory cilia are present on the dendritic endings of 60/302 neurons of the *C. elegans* adult worm (Collet et al., 1998; Perkins et al., 1986); of these 60 ciliated neurons, 26 are thought to be chemosensory, as their terminal sensory cilia are open to the external environment. This includes the amphid and inner labial neurons of the head, and the phasmid neurons of the tail (Perkins et al., 1986; Ward et al., 1975; Starich et al., 1995). The chemosensory cilia act as specialized compartments to concentrate receptors and other signaling molecules responsible for detecting environmental stimuli that control at least five distinct behaviors including chemotaxis, osmotic avoidance, egg laying, mating, and dauer larva formation (Perkins et al., 1986; Chalfie and White, 1988; Chou et al., 1996; Dwyer, 1998).

There are two heteromeric kinesin complexes in *C. elegans*: heterotrimeric kinesin-II and dimeric Osm-3–kinesin (Signor et al., 1999). Kinesin-II is most homologous in sequence and subunit composition to members of the heteromeric subfamily in other organisms, including the prototypic heterotrimeric kinesin-II in sea urchin and the heterotrimeric FLA-10 kinesin-II in *Chlamydomonas* (Signor et al., 1999). Both complexes are expressed in chemosensory neurons and concentrate in sensory cilia (Signor et al., 1999). The dimeric Osm-3–kinesin complex contains the motor subunit OSM-3, which is known to be important in the formation and/or maintenance of sensory cilia (Shakir et al., 1993; Tabish et al., 1995; Perkins et al., 1986). *osm-3* mutants demonstrate defects in several behaviors including osmotic avoidance because they lack the distal portions of their sensory cilia (Perkins et al., 1986; Starich et al., 1995). Heterotrimeric kinesin-II has been hypothesized to be involved in the anterograde transport of the *C. elegans* protein OSM-6 within amphid sensory cilia, as GFP-tagged OSM-6 and the kinesin-II accessory polypeptide (KAP) move at similar rates toward the distal tips of sensory cilia in vivo (Orozco et al., 1999), and because OSM-6 is a homologue of one of the raft components identified in *Chlamydomonas* (Cole et al., 1998; Collet et al., 1998). OSM-6::GFP fusion proteins are expressed exclusively in sensory neurons, and like the heteromeric kinesins, kinesin-II and Osm-3–kinesin, localize to sensory cilia (Collet et al., 1998).

The *osm-6* mutant is one of ~100 mutations in 25 genes that have been identified in various behavioral screens that demonstrate defects in sensory function (Dusenbery et al., 1975; Lewis and Hodgkin, 1977; Culotti and Russell, 1978; Riddle et al., 1981; Starich et al., 1995). Most of these mutants are defective in chemosensory behavior because of structural abnormalities in their ciliary axonemes (Lewis and Hodgkin, 1977; Perkins et al., 1986; Starich et al., 1995). Another mutant, *osm-1*, shares similar phenotypic traits with *osm-6*, characterized by severely truncated sensory cilia and ectopic assembly of microtubules and axonemal structures proximal to the transition zone (Perkins et al., 1986; Starich et al., 1995). The OSM-1 protein also has been identified as a likely homologue of another IFT raft polypeptide found in *Chlamydomonas* flagella (Cole et al., 1998; Stone, Steven, and Jocelyn Shaw, personal communication), and may represent a second component of the kinesin-II cargo complex.

In this study, we use a time-lapse fluorescence microscopic transport assay (Orozco et al., 1999) to visualize kinesin-II, OSM-1, and OSM-6, moving retrogradely along cilia and dendrites. These proteins moved at the same rate, consistent with the hypothesis that they are retrieved by a shared retrograde transport pathway that moves them back to the cell body. We provide evidence that the CHE-3

cytoplasmic dynein motor is responsible for the retrograde transport of kinesin-II and its cargo within sensory cilia, but is not required for retrograde transport of these molecules in the corresponding dendrites. This may be the first evidence that a cytoplasmic dynein functions in a specific subcellular compartment during retrograde traffic in neurons.

Materials and Methods

Identification and Characterization of the osm-1 Gene and Predicted Open Reading Frame (ORF)

Cosmids spanning the region where the *osm-1* mutation has been previously mapped were analyzed for ORFs that may encode the 20–amino acid peptide previously reported to be part of the OSM-1 protein (Cole et al., 1998; Stone, Steven, and Jocelyn Shaw, personal communication). Overlapping cosmids were identified using AceDB software, and their sequences were obtained through NCBI GenBank. All predicted ORFs on cosmids T25D1, T27B1, K08B5, F59C12, and C06G1 (provided by Dr. Alan Coulson, Sanger Center, Cambridge, UK) were analyzed for their inclusion of the 20–amino acid peptide sequence that is conserved in both *C. elegans* and *Chlamydomonas* homologues of OSM-1 (Stone, Steven, and Jocelyn Shaw, personal communication; Cole et al., 1998). The peptide was localized to ORF T27B1.1, but the cosmid was found to contain a deletion upon restriction enzyme analysis. The overlapping cosmid C15H5 was used instead for subsequent subcloning. The predicted OSM-1 polypeptide sequence was analyzed for sequence motifs and predicted domains using various algorithms provided on the ExPASy homepage, proteomics tools (http://www.expasy.ch).

Construction of the OSM-1::GFP Rescue Construct

The *osm-1* gene and upstream regulatory sequences were subcloned into the pPD95.77 GFP genomic transformation vector provided by Dr. Andrew Fire (Carnegie Institute of Washington, Baltimore, MD) using standard molecular biology protocols (Sambrook et al., 1989). Specifically, a 3.1-kb *osm-1* gene fragment representing the most 3′ end of the *osm-1* gene was PCR amplified from cosmid C15H5 using the primers 5′-ttggatcctctgcgtctcttatccc-3′ and 5′-caatcccggggacaacgaaatagccaacgg-3′ (SmaI site underlined; added to facilitate the in-frame ligation of *osm-1* to GFP). This 3.1-kb fragment was shuttled through PCR-Blunt (Invitrogen Corp.) and ligated into pPD95.77 using BamHI and SmaI sites. Then, an SphI-BamHI 5.2-kb fragment representing the 5′ end of the osm-1 gene plus 2.5 kb of upstream sequence was excised from cosmid C15H5 and added to the aforementioned pPD95.77 vector containing the 3.1-kb 3′ end fragment. Finally, a BamHI-BglII 3.8-kb genomic fragment representing the middle of the osm-1 gene was added into the pPD95.77 vector containing the 5.2- and 3.1-kb fragments, fully reconstituting the entire *osm-1* gene (9.7 kb) plus 2.5 kb of upstream promoter sequence.

Transgenics and Mutants

Heritable lines of transgenic worms carrying extrachromosomal arrays of OSM-1::GFP–encoding constructs were created by coinjection of the aforementioned *osm-1*/pPD95.77, and plasmid pRF4 containing the semidominant marker mutation *rol-6(su1006)*, into homozygous *osm-1 (p808)* (Culotti and Russell, 1978) hermaphrodites by methods previously described (Fire, 1986; Kramer et al., 1990; Mello et al., 1991). Heritable roller lines were selected, and rescue of the *osm-1* mutant phenotype was assayed by dye filling as previously described (Perkins et al., 1986; Starich et al., 1995). The uptake of DiI into amphid and phasmid chemosensory neurons was monitored by epifluorescence microscopy.

Heritable lines carrying GFP-tagged kinesin-II accessory polypeptide (KAP::GFP, strain 12.5) were made by similar methods and described previously (Orozco et al., 1999; Signor et al., 1999). OSM-6::GFP worms were provided by Drs. Jocelyn Shaw and Robert K. Hermann (University of Minnesota, St. Paul, MN). Males expressing OSM-6::GFP or KAP::GFP were crossed with homozygous mutant *che-3* or *osm-3* hermaphrodites, and the F1 heterozygotes were selfed to obtain OSM-6::GFP;*che-3*, OSM-6::GFP;*osm-3*; and KAP::GFP;*che-3* progeny (Brenner, 1974). *Che-3* and *osm-3* homozygosity was verified by dye filling. We were unable to create OSM-1::GFP;*che-3* progeny because of the low male mating efficiency characteristic of roller mutants. The progeny of these crosses were scored for fusion protein expression patterns by laser scanning confocal microscopy and in vivo transport by methods described below. The *che-3 (e1124)* (Lewis and Hodgkin, 1977), *osm-1 (p808)* (Culotti and Russell, 1978), and *osm-3 (p802)* (Culotti and Russell, 1978) strains were obtained through the *Caenorhabditis* Genetics Center (University of Minnesota, St. Paul, MN). For transport assays, one strain expressing OSM-6::GFP was used (Sp2101), one strain expressing KAP::GFP was used (12.5), and two strains expressing OSM-1::GFP were used (SL16 and SL17).

In Vivo Transport Assay

Adult transgenic worms expressing translational fusions of OSM-1::GFP, OSM-6::GFP, and KAP::GFP were assayed for in vivo transport by time-lapse fluorescence microscopy. Specifically, GFP-expressing worms were anesthetized with 10 mM Levamisole and mounted onto poly-L-lysine–coated slides. Paralyzed, nontwitching worms were selected using bright field microscopy at 10×, and transport was visualized by collecting fluorescent images at 100× at 1 frame per second or 1 frame per 0.5 s intervals using a Nikon Eclipse E600 microscope equipped with a Uniblitz automated shutter driver and Metamorph Imaging System software (Universal Imaging Corp.). Images were collected for a minimum of 1 min, and movies were created from stacked images using Metamorph Imaging software. Still images were taken from individual frames of time-lapse collections.

We routinely used 10 mM Levamisole (rather than the 1 mM concentration that is often used with *C. elegans)* to completely inhibit twitching and, thus, to facilitate microscopic observations of transport. In control experiments, we found that rates of transport were identical in 1 and 10 mM Levamisole (e.g., in 1 mM Levamisole, OSM-6::GFP particles were observed to move at 0.65 ± 0.06 μm/s anterogradely [10 animals, 52 GFP particles], and 1.08 ± 0.07 μm/s retrogradely [10 animals, 30 GFP particles]). Moreover, we found that the paralyzing effects of the anesthetic are reversible at both concentrations; worms treated with 1 or 10 mM Levamisole for periods of time corresponding to the length of typical transport assays completely recover movement within 24 h of being transferred to anesthetic-free buffer.

Velocities of transport were determined by analyzing time-lapse transport movies for moving dots of fluorescence. The relative positions of individual fluorescent particles were monitored over multiple frames (≥4) and velocities were calculated by determining total distance moved per given time period using an objective micrometer. Anterograde IFT movement was designated as the movement of fluorescent particles from the transition zone of sensory cilia toward the ciliary endings at the tip/nose of the worm; retrograde transport was designated as movement of fluorescent particles from the tip back toward the transition zone (see Fig. 1). Bidirectional movement of GFP particles was also analyzed in associated dendrites of amphid and phasmid chemosensory neurons, with anterograde intradendritic transport corresponding to the movement of GFP particles from the cell body toward the transition zone, and retrograde intradendritic transport as the movement back toward the cell body (see Fig. 1).

Results

We previously used a time-lapse fluorescence microscope–based transport assay to visualize the anterograde movement of kinesin-II::GFP (labeled on the KAP subunit) and OSM-6::GFP within sensory cilia (but not dendrites) of amphid chemosensory neurons in living transgenic *C. elegans* (Fig. 1 c, step 2; Orozco et al., 1999). However, in that study, we were unable to visualize the retrograde transport of these IFT motors and raft particles, which left unanswered the question of whether these proteins are moved back along the cilia and dendrites by a retrograde retrieval pathway (Fig. 1 c, steps 3 and 4), or if instead they are degraded and rendered nonfluorescent at the distal tip of the cilia. Here, we show that kinesin-II and its cargo molecules do in fact move in the retrograde direction as well as the anterograde direction in both dendrites and cilia of amphid and phasmid chemosensory neurons (Fig. 1). Moreover, we have extended our analysis to a second pre-

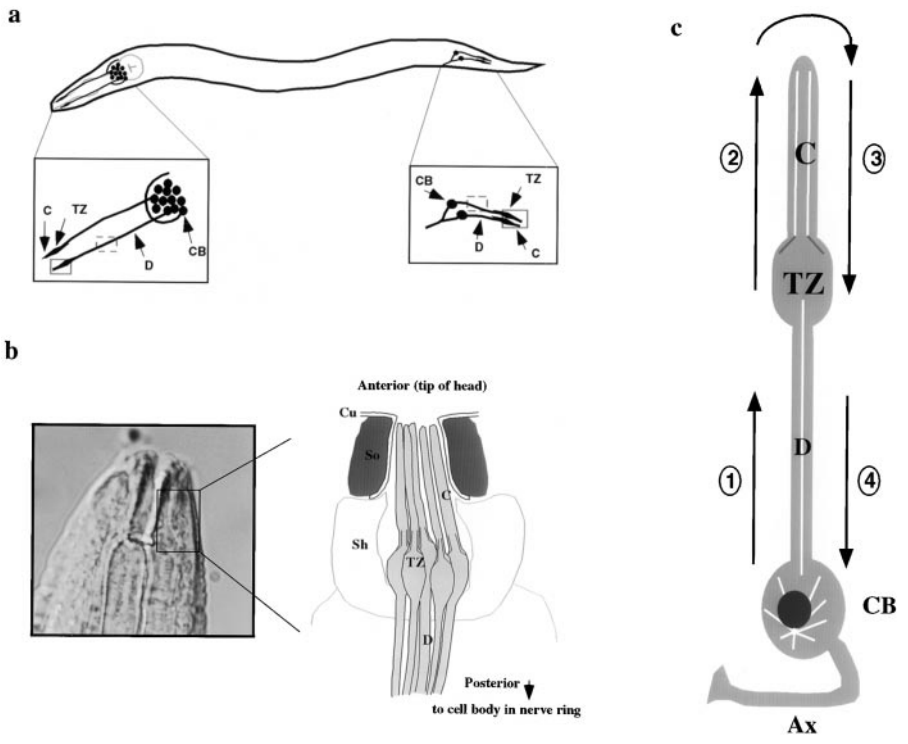

Figure 1. (a) Schematic representation of the amphid and phasmid chemosensory neurons indicating the regions monitored for in vivo transport of GFP fusion proteins. Shown is a simplified view of an adult wild-type worm with amphid neuron cell bodies and corresponding dendrites in the head, and phasmid neuron cell bodies and corresponding dendrites in the tail. Insets show a close-up view of the areas monitored for bidirectional IFT transport in ciliated endings (solid box), and bidirectional dendritic transport (dashed box). (b) Diagram showing high magnification view of an amphid sensillum. The diagram represents a transverse section through the amphid channel, which is located at the tip of the head, and normally contains eight ciliated amphid neurons that are open to the external environment through a pore in the cuticle (five are shown for simplicity; adapted from Perkins et al., 1986). (c) High magnification view of a single ciliated amphid neuron demonstrating the four classes of transport being studied: (1) anterograde intradendritic transport from the cell body toward the transition zone of the sensory cilium; (2) anterograde intraflagellar transport from the base of the transition zone toward the tip of the cilium; (3) retrograde intraflagellar transport from the tip of the cilium back toward the transition zone; and (4) retrograde intradendritic transport from the base of the transition zone back toward the cell body. For all: shown are the transition zones (TZ) and sensory cilia (C) that comprise the terminal endings of these chemosensory neurons, and the cell bodies (CB) and corresponding dendrites (D). Also shown in b are the cuticle (Cu) and Socket (So) and Sheath (Sh) supporting cells, and in c, the cell body (CB) and axon (Ax).

sumptive cargo molecule, OSM-1, which required the production of OSM-1::GFP–expressing transgenic lines.

Characterization of OSM-1::GFP Transgenic Worms

Previous work showed that the *osm-1* gene is essential for the formation and/or maintenance of chemosensory cilia that detect chemosensory cues, and that *osm-1* mutants display defects in ciliary structure resulting in defects in fluorescent dye-filling ability and osmotic avoidance behavior (Perkins et al., 1986; Starich et al., 1995; Stone, Steven, and Jocelyn Shaw, personal communication). The OSM-1 protein is encoded by ORF T27B1.1 on genomic cosmid T27B1 (GenBank accession number U41020). To study the transport of the OSM-1 protein within dendrites and cilia of chemosensory neurons, we constructed transgenic lines carrying extrachromosomal arrays of constructs driving the expression of an OSM-1::GFP fusion protein under the control of the endogenous *osm-1* promoter. Specifically, a 12.1-kb genomic fragment that included the *osm-1* gene and 2.5 kb of upstream sequences were placed in-frame with the GFP gene in a *C. elegans* transformation vector and injected into the *osm-1* homozygous mutant background.

In the *osm-1* mutant, defects in sensory ciliary structure give rise to corresponding defects in the uptake of fluorescent dyes such as DiI into six pairs of amphid channel neurons in the head and two pairs of phasmid channel neurons in the tail (Perkins et al., 1986; Starich et al., 1995). The OSM-1::GFP fusion protein appears to be functional as it rescues the *osm-1* mutant phenotype as demonstrated by the restoration of the dye-filling ability (Fig. 2).

Bidirectional Transport of Kinesin-II Motors and Cargo along Sensory Cilia

Initially, it was only possible to clearly visualize anterograde IFT in sensory cilia (Orozco et al., 1999), but we are now able to readily visualize retrograde transport as well. Thus, we observed the bidirectional transport of kinesin-II and its presumptive cargo in vivo within the sensory ciliary regions indicated in steps 2 and 3 of Fig. 1 c, by time-lapse fluorescence microscopy of adult transgenic worms expressing KAP::GFP, OSM-1::GFP, and OSM-6::GFP fusion proteins. All three GFP fusion proteins are expressed in amphid and phasmid chemosensory neurons, where they appear to concentrate at the base of the transition zones, which correspond to the basal bodies of motile and sensory cilia. These fusion proteins are seen to emerge from the transition zones as small fluorescent particles that move in a bidirectional fashion along the sensory cilia, displaying anterograde movement from the transition zone toward the tip of the ciliary axoneme (Fig. 3) and retrograde movement from the cilium tip back toward the transition zone (Fig. 4).

The average velocities of intraflagellar transport of

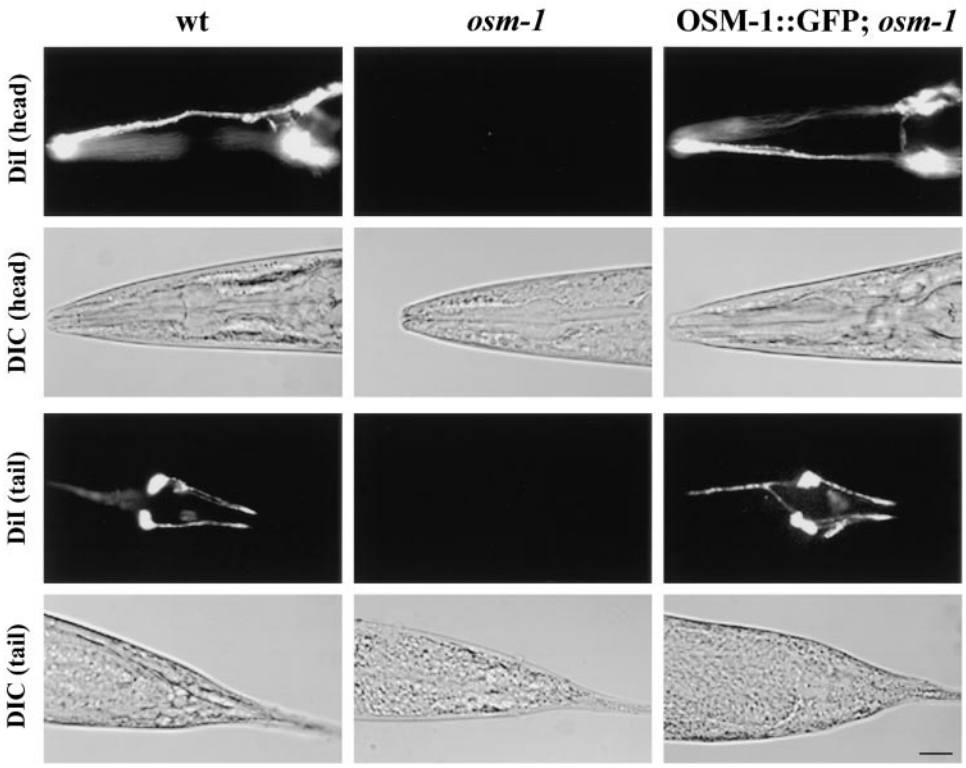

Figure 2. Rescue of the *osm-1* mutant phenotype with the OSM-1::GFP fusion construct. Rescue of the *osm-1* mutant phenotype is demonstrated by the ability of wild-type and transgenic worms to fill with the fluorescent dye DiI. *osm-1* mutant worms are unable to dye fill because of structural defects in their amphid neuron sensory cilia. Top two rows demonstrate dye filling of the amphid chemosensory neurons of the head and corresponding DIC image; bottom two rows demonstrate dye filling of the phasmid chemosensory neurons of the tail and corresponding DIC image. Bar, 10 μm.

OSM-1::GFP, OSM-6::GFP, and KAP::GFP, were very similar in a given direction (Table I), although the average rates differed between anterograde and retrograde IFT (Table I). The average rates of anterograde transport were ~0.7 μm/s for these three proteins, which agree with the rates reported previously for OSM-6::GFP and KAP::GFP in sensory cilia (Orozco et al., 1999). The retrograde transport velocities of OSM-1::GFP, OSM-6::

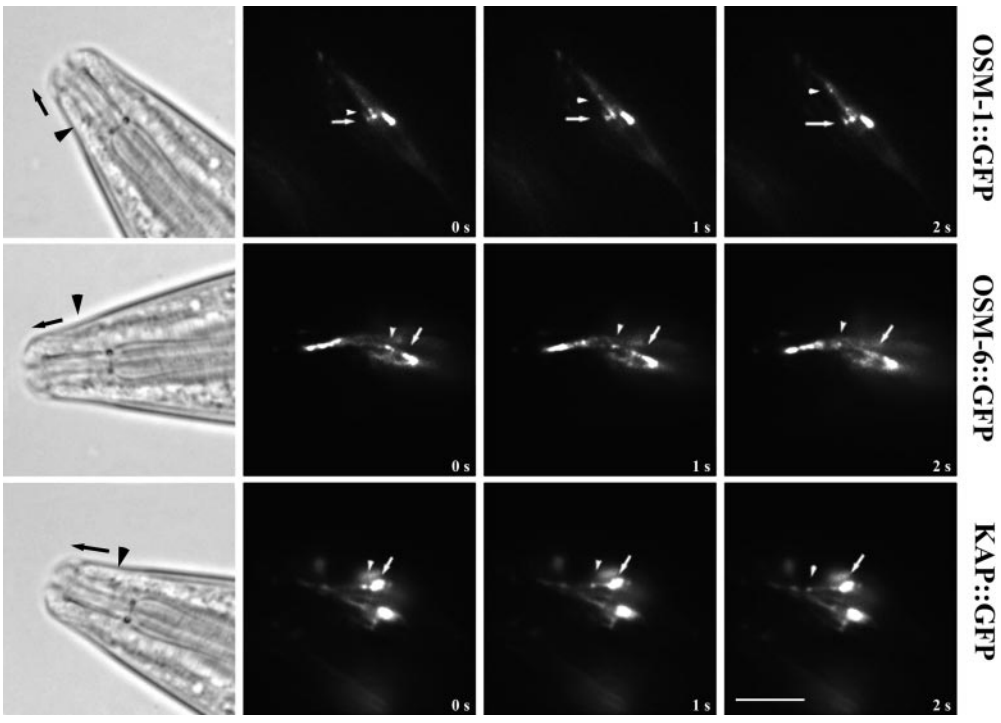

Figure 3. Anterograde IFT transport of kinesin-II and presumptive cargo molecules in chemosensory cilia. Transgenic lines of worms expressing translational fusions of OSM-1, OSM-6, and KAP fused to GFP were assayed for anterograde IFT transport in vivo using time-lapse fluorescence microscopy. OSM-1::GFP, OSM-6::GFP, and KAP::GFP all accumulate in the transition zones at the base of the sensory cilia, and IFT rafts (GFP particles) are seen moving outward from these zones toward the tip of the cilium. Arrows point to fixed areas of fluorescence in the transition zones, arrowheads point to moving GFP particles. DIC images of a generic wild-type worm are provided for orientation, with arrowheads pointing to areas corresponding to the transition zones, and arrows demonstrating direction of movement. Bar, 5 μm.

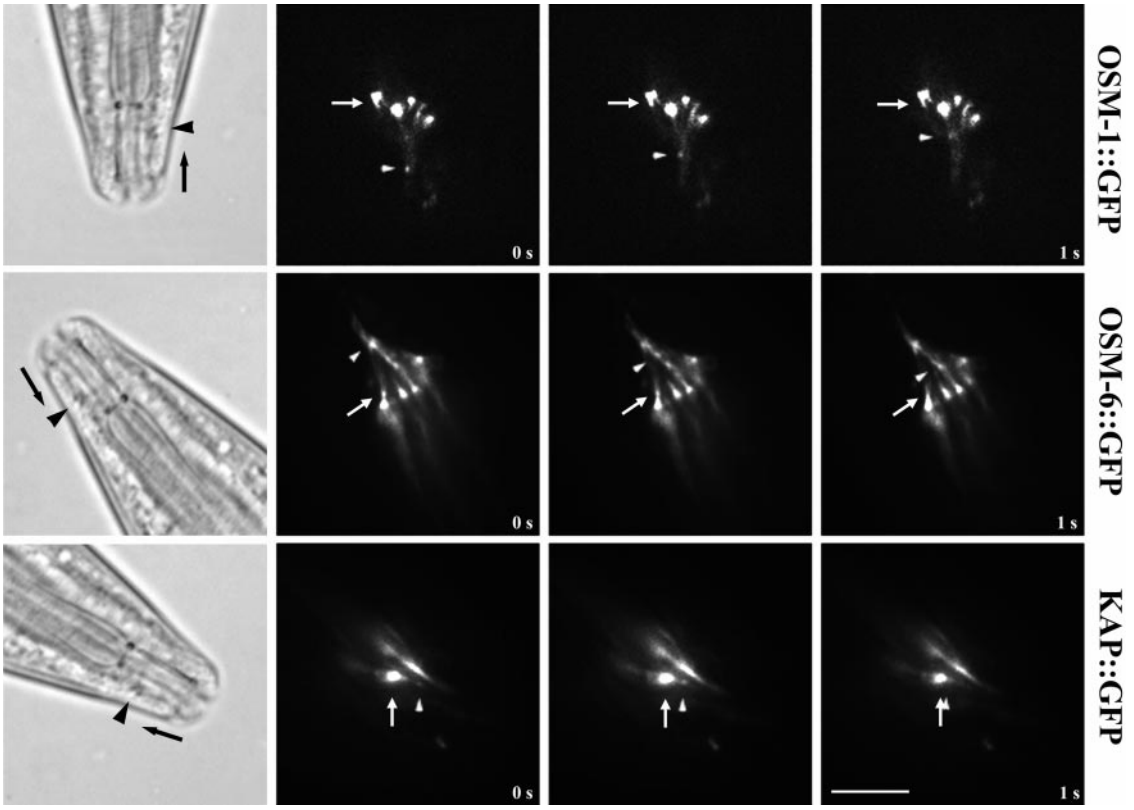

Figure 4. Retrograde IFT transport of kinesin-II and presumptive cargo molecules in sensory cilia. Worms expressing OSM-1::GFP, OSM-6::GFP, and KAP::GFP were assayed for retrograde transport in sensory cilia using methods discussed in Fig. 3. The retrograde movement of these molecules is seen as the movement of fluorescent particles from the tip of the sensory cilium toward the transition zone. Arrows point to fixed areas of fluorescence in the transition zones, arrowheads point to moving GFP particles. Bar, 5 μm.

GFP, and KAP::GFP within sensory cilia were also similar (Table I); average rates of retrograde transport were ~1.10 μm/sec, which is consistent with the hypothesis that the retrograde IFT transport pathway is shared between these molecules.

Bidirectional Transport of Kinesin-II Motors and Cargo along Dendrites

We observed the bidirectional transport of KAP::GFP, OSM-1::GFP, and OSM-6::GFP in dendritic segments of amphid and phasmid chemosensory neurons (Fig. 1 c, steps 1 and 4, and Fig. 5). The rates of anterograde movement (corresponding to the movement of GFP particles from the cell body along the dendrite toward the transition zone of sensory cilia) and retrograde transport (corresponding to the movement of GFP particles from the transition zone along the dendrite back toward the cell body) were very similar for all three GFP fusion proteins (Fig. 5 and Table II). Specifically, KAP::GFP, OSM-1::GFP, and OSM-6::GFP showed average rates of anterograde dendritic transport of ~0.7 μm/sec and average retrograde transport rates of ~1.0 μm/sec. These velocities are essentially the same as those measured in sensory cilia. In all transgenic worms examined, nonmoving GFP particles were seen along the dendrites. Because these fluorescent spots were of various sizes and immotile, they are likely to be GFP aggregates that have formed within the cell.

Table I. Bidirectional Transport Velocities of IFT Components along Sensory Cilia

Transgenic strain (No. animals)	Average velocity			
	Anterograde	(N)	Retrograde	(N)
	$\mu m\ s^{-1}$		$\mu m\ s^{-1}$	
OSM-1::GFP (21)	0.67 ± 0.10	(135)	1.10 ± 0.14	(125)
OSM-6::GFP (28)	0.68 ± 0.11	(201)	1.08 ± 0.16	(100)
KAP::GFP (17)	0.67 ± 0.09	(115)	1.07 ± 0.10	(31)

(N) = No. of GFP particles.

Table II. Bidirectional Transport Velocities of Kinesin-II and Presumptive Cargoes along Dendrites

Transgenic strain (No. animals)	Average velocity			
	Anterograde	(N)	Retrograde	(N)
	$\mu m\ s^{-1}$		$\mu m\ s^{-1}$	
OSM-1::GFP (14)	0.71 ± 0.07	(40)	1.04 ± 0.08	(40)
OSM-6::GFP (12)	0.75 ± 0.10	(60)	1.02 ± 0.10	(60)
KAP::GFP (23)	0.71 ± 0.08	(102)	1.01 ± 0.14	(100)

(N) = No. of GFP particles.

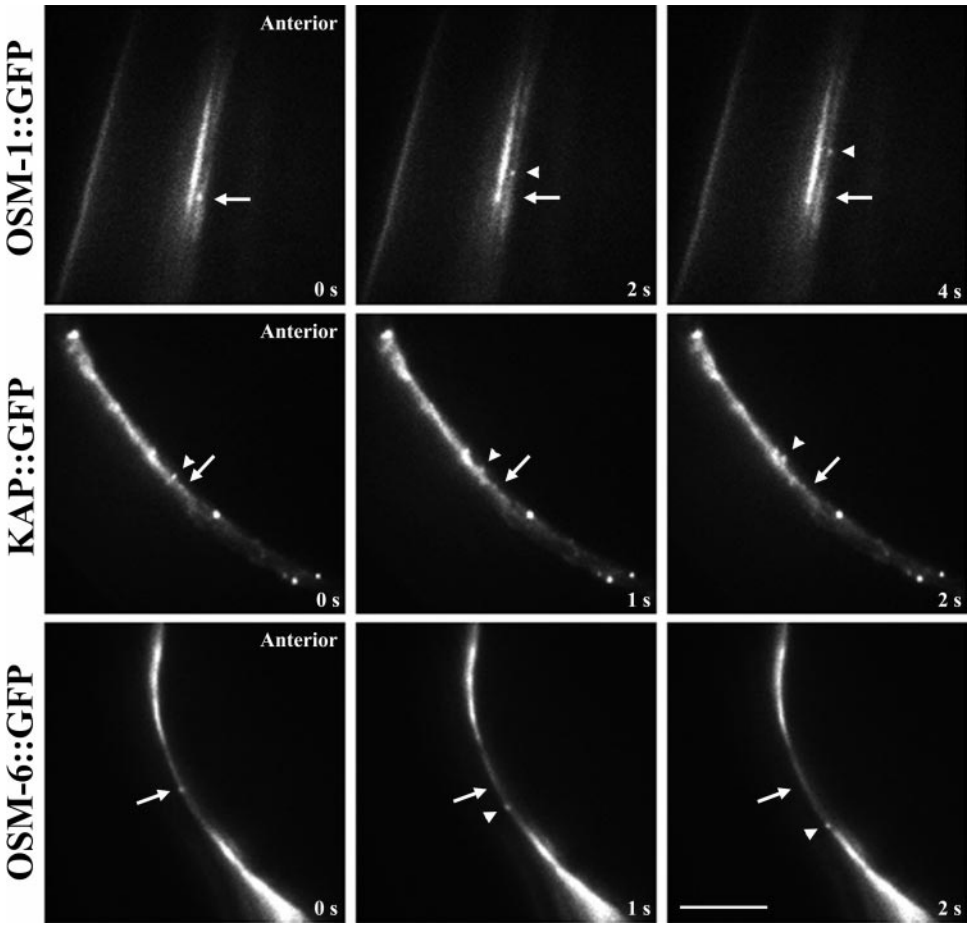

Figure 5. Bidirectional dendritic transport of kinesin-II and presumptive cargo molecules in sensory neurons. The anterograde and retrograde transport of OSM-1::GFP, OSM-6::GFP, and KAP::GFP were assayed in amphid chemosensory neuron dendrites in vivo as the movement of GFP particles toward the transition zone and sensory cilia or toward the cell body, respectively. All three fusion proteins demonstrate bidirectional transport in amphid neuron dendrites. Anterograde transport of OSM-1::GFP and KAP::GFP are shown in the top two rows, with the transition zones and sensory cilia located anteriorly; retrograde transport of OSM-6::GFP is demonstrated in the bottom row, with the associated cell body located posteriorly. Arrows point to fixed regions along the dendrite for orientation, arrowheads point to moving GFP particles. Bar, 5 μm.

Specific Inhibition of Retrograde Intraflagellar Transport but Not Intradendritic Transport in che-3 Cytoplasmic Dynein Mutants

To investigate whether the CHE-3 cytoplasmic dynein drives the retrograde transport of kinesin-II and its presumptive cargo protein, OSM-6, within sensory cilia, we expressed the KAP::GFP and OSM-6::GFP fusion proteins in a *che-3* homozygous mutant background and assayed for transport by time-lapse fluorescence microscopy.

The *che-3 (e1124)* reference allele, which we used here, has been sequenced and found to contain a premature ochre stop codon approximately halfway through the predicted protein sequence (codons CAA to TAA, Q2233STOP; Wicks, S., C. deVries, H. Van Luenen, and R. Plasterk, manuscript submitted for publication). This truncates the heavy chain at the first amino acid after the third P-loop, which is conserved in all dyneins, eliminating much of the catalytic domain and rendering *che-3 (e1124)* a strong candidate null or severe loss-of-function mutation (Wicks, S., C. deVries, H. Van Luenen, and R. Plasterk, manuscript submitted for publication). This conclusion is supported by the observation that *che-3 (e1124)* over three separate deficiencies is phenotypically the same as *che-3 (e1124)* homozygotes (Starich et al., 1995). Genomic cosmid F18C12 encodes the DHC1b orthologue, CHE-3, and this completely rescues the *che-3 (e1124)* mutant phenotype based on microscopy observations of ciliary morphology and assays for dye filling and chemotaxis behavior (Wicks, S., C. deVries, H. Van Luenen, and R. Plasterk, manuscript submitted for publication; Grant, W., personal communication). The *che-3* ORF, F18C12.1 (GenBank accession number Z75536), predicts a 4,131–amino acid DHC1b polypeptide that, when compared to other proteins in the GenBank sequence database including multiple dynein heavy chains, shares highest homology (44% identity, 54% similarity in the region corresponding to amino acids 898–2,071 of CHE-3) with partial cDNA sequence encoding DHC1b in *Chlamydomonas* (GenBank accession number AF096277).

Strikingly, over many hours of observation, we never saw retrograde IFT in cilia of *che-3* mutants, in contrast to the robust transport that we consistently observed in wild-type worms. This inhibition was specific for retrograde IFT (Fig. 1 c, step 3) since we observed that anterograde IFT continued unabated in the shortened cilium of *che-3* mutants. Accordingly, we observed an accumulation of both KAP::GFP and OSM-6::GFP at the distal tips of the slightly truncated cilia in *che-3* mutants, compared with the normal enrichment of these fusion proteins in the transition zones of wild-type worms (Fig. 6), presumably because of the continuous anterograde movement of OSM-6::GFP and kinesin-II to the distal tip of cilia, but defective retrieval. This accrual of fluorescence at cilia tips was obvious in the amphid sensory cilia of the head and phasmid sensory cilia of the tail (Fig. 6).

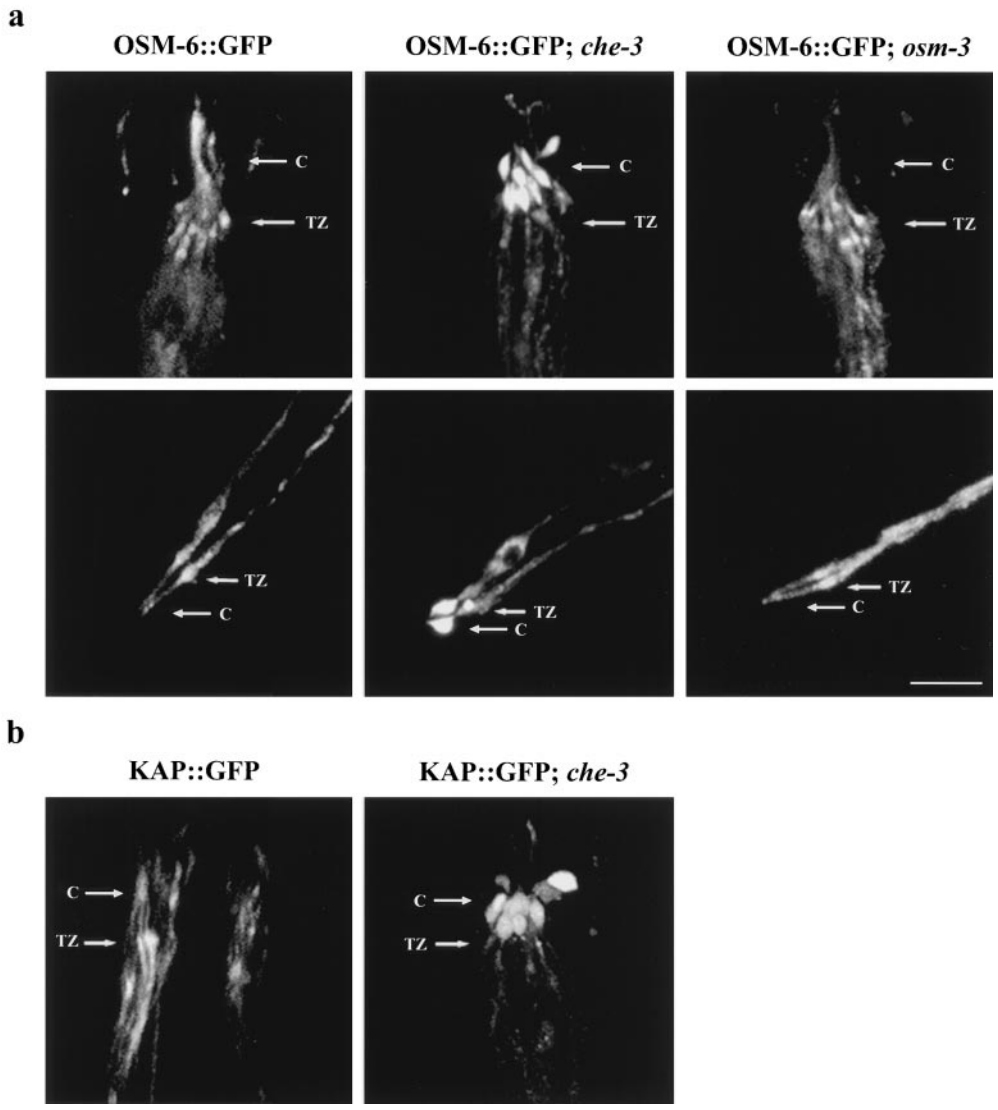

Figure 6. Mislocalization of OSM-6 and KAP in the cytoplasmic dynein mutant *che-3*. Homozygous *che-3* mutant worms expressing OSM-6::GFP and KAP::GFP were examined for fluorescence localization by confocal microscopy. Arrows point to regions corresponding to the transition zones (TZ) and sensory cilia (C). (a, top row) OSM-6::GFP shows normal accumulation in the transition zones of the amphid chemosensory neurons and diffuse fluorescence along the sensory cilia in wild-type worms and in the *osm-3* mutant background, but accumulates at the tips of the truncated sensory cilia in the *che-3* mutant background. (bottom row) Similar defects in OSM-6::GFP localization are seen in phasmid chemosensory neurons of the tail, where OSM-6::GFP accumulates normally in the transition zones in wild-type and *osm-3* mutant backgrounds, but accumulates abnormally as large fluorescent bulbs at the tips of the sensory cilia in worms lacking the CHE-3 cytoplasmic dynein. (b) KAP::GFP also accumulates abnormally at the tips of sensory cilia in amphid chemosensory neurons. Bar, 5 μm.

The fact that anterograde IFT persists in *che-3* mutant animals suggests that the inhibition of retrograde transport does not reflect a nonspecific disruption of transport in general. To further address whether the inhibition of retrograde transport seen in the sensory cilia was an indirect, nonspecific effect of having an abnormal, truncated axoneme, we monitored OSM-6::GFP expression and transport in the *osm-3* mutant background. The *che-3* and *osm-3* mutants have similar axonemal defects; both are missing the distal segments of the axoneme, but retain their middle and proximal segments (Lewis and Hodgkin, 1977; Perkins et al., 1986). *che-3* differs from *osm-3* in that the middle segments of its cilia have swollen tips (Lewis and Hodgkin, 1977). Using confocal microscopy, we compared the ciliary defects of *osm-3* and *che-3* and estimated that both are missing the distal 2.5 μm of their axoneme, with *che-3* missing an additional 0.8 μm from its middle segment. Thus, the *che-3* dynein mutant retains ~4.2 μm of the middle and proximal segments of their axoneme, of which 1.6 μm is bulbous in nature and the other 2.6 μm appears normal and visibly supports anterograde transport. Bidirectional transport of OSM-6::GFP was normal in the shortened cilia of the *osm-3* mutant (0.66 ± 0.07 μm/s anterogradely, 1.09 ± 0.09 μm/s retrogradely), and the OSM-6::GFP fusion protein demonstrated normal localization to the transition zones and cilia (Fig. 6). These results argue that the type of inhibition of retrograde transport seen in *che-3* mutants is not seen in all structurally abnormal cilia, which is consistent with it being a specific effect.

To determine if CHE-3 cytoplasmic dynein was also responsible for the retrograde intradendritic transport of kinesin-II and its presumptive cargoes from the sensory cilia back to the cell body, we analyzed the transport of the KAP::GFP and OSM-6::GFP fusion proteins in sensory neuronal dendrites in the *che-3* homozygous mutant background (Fig. 7). Although these fusion proteins show dramatic accumulation at the tips of both amphid and phasmid sensory cilia because of defects in retrograde IFT along the ciliary axoneme, the retrograde transport of these proteins from the transition zone back toward the cell body occurs normally in the corresponding dendrite (Fig. 7 and Table III). The retrograde transport of KAP::GFP and OSM-6::GFP in *che-3* mutant amphid dendrites occurred at an average velocity of ~1.0 μm/s in both cases

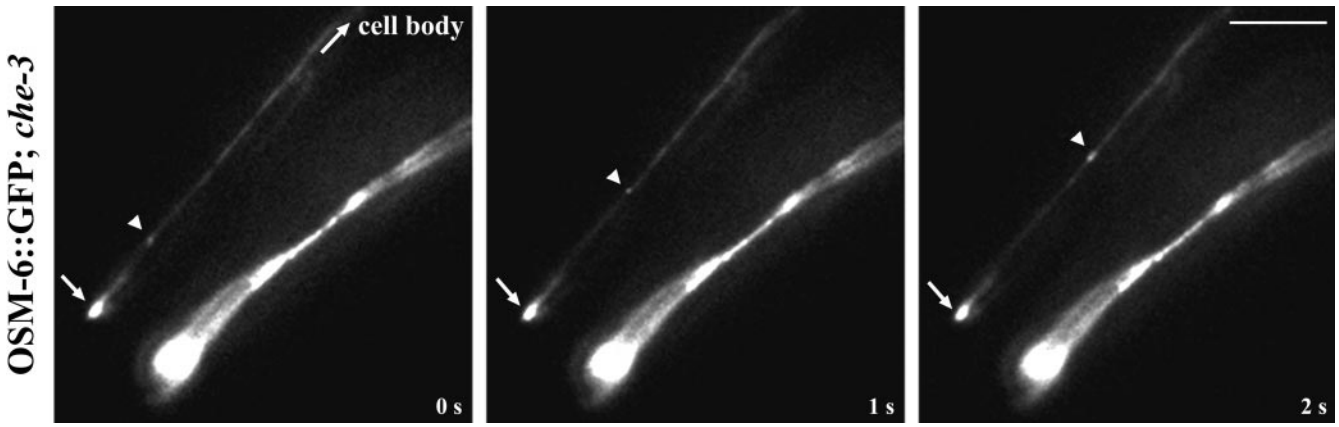

Figure 7. Retrograde transport of OSM-6::GFP occurs normally in dendrites lacking the CHE-3 cytoplasmic dynein. Homozygous *che-3* mutants expressing the OSM-6::GFP fusion protein were examined for transport in sensory cilia and their corresponding dendrites. Shown are phasmid chemosensory neurons of the tail with an accumulation of OSM-6::GFP fusion protein at the tips of the sensory cilia (arrow), and diffuse protein along the corresponding dendrite back toward the cell body. Retrograde transport of OSM-6::GFP is defective in sensory cilia of *che-3* mutants, but occurs normally in the corresponding dendrite (arrowheads). Bar, 5 μm.

(Table III), which is similar to their retrograde transport velocities in wild-type backgrounds. Thus, CHE-3 dynein appears to be involved specifically in retrograde IFT (Fig. 1 c, step 3).

Discussion

This paper, together with our previous study (Orozco et al., 1999), documents the use of a fluorescence microscope–based transport assay to observe the bidirectional movement of a motor, heterotrimeric kinesin-II, and two proteins that are essential for sensory ciliary function, OSM-1 and OSM-6, along cilia and dendrites within chemosensory neurons of living *C. elegans*. Previously, we observed anterograde movement of these molecules along cilia (Orozco et al., 1999), but retrograde transport was not observed. Improvements in the assay have allowed us to show in the current study that these molecules are indeed moved along cilia and dendrites in a retrograde direction at the same rate, which may reflect the operation of a retrieval pathway for IFT motors and IFT rafts. Moreover, through the use of a *che-3* dynein motor mutant, we obtained results that are consistent with the hypothesis that CHE-3 dynein participates in the early phase of retrieval of the anterograde motor, heterotrimeric kinesin-II, and its presumptive cargo molecules by moving these proteins from the distal tip of the ciliary axoneme back to the transition zone (Fig. 1 c, step 3). However, the later phases of retrograde transport of these IFT proteins appear to depend on a different motor that drives retrograde intradendritic transport.

Table III. Retrograde Dendritic Transport Velocities in che-3 Mutants

Transgenic strain (No. animals)	Average velocity	(N)
	$\mu m\ s^{-1}$	
OSM-6::GFP (15)	1.04 ± 0.11	(45)
KAP::GFP (12)	1.02 ± 0.08	(40)

(N) = No. of GFP particles.

What Are the Functions of This Transport System?

It is plausible that the transport system that we are characterizing serves to transport key neuronal components from their site of synthesis in the cell body, out along the dendrite, to the distal tip of the sensory cilium. Such components could include chemosensory receptors and other sensory signaling molecules that are concentrated in sensory cilia as well as structural components of ciliary axonemes. The observation that mutations in two components of this transport pathway, OSM-1 and OSM-6, cause defects in both sensory ciliary structure and chemosensory behavior supports this hypothesis.

OSM-1 and OSM-6 proteins are members of a set of ~25 genes that are required for sensory ciliary structure and function in *C. elegans*. (Starich et al., 1995). Both the *osm-1* and *osm-6* mutants were identified in a screen for osmotic avoidance defective behavior (Culotti and Russell, 1978; Hedgecock et al., 1985). Both are dye filling defective and have structural abnormalities in axonemes of their chemosensory cilia that cause defects in other behaviors such as chemotaxis and thermotaxis (Culotti and Russell, 1978; Hedgecock et al., 1985; Perkins et al., 1986; Starich et al., 1995). The *osm-6* mutant was cloned and characterized by Collet et al. (1998) and the *osm-1* mutant was cloned by Jocelyn Shaw and Stephen Stone (personal communication). The predicted ORF for OSM-1 (T27B1.1) suggests that OSM-1 is a novel, large molecular weight protein with no obvious motifs or transmembrane domains, which is consistent with the hypothesis that OSM-1 is a nonmembrane-bound component of IFT raft particles (Cole et al., 1998).

The OSM-1 and OSM-6 polypeptides are proposed to be components of *C. elegans* IFT raft particles that convey structural components such as axonemal precursors that are required for ciliary assembly and/or maintenance (Cole et al., 1998). The precise functions of the OSM-1 and

OSM-6 proteins are unclear, but they may act as carriers of cargo, or may play a more direct role in axonemal assembly, such as chaperones or structural components of axonemes. The severely shortened axonemes and ectopic microtubule assembly characteristic of *osm-1* and *osm-6* mutants would be consistent with such roles in ciliary assembly.

Alternatively, OSM-1 and OSM-6 may represent signaling molecules that are localized to sensory cilia, and are involved in the reception/integration pathway(s) of environmental stimuli, similar to receptor molecules that are transported from the cell body to their site of action in sensory cilia (Bargmann et al., 1990; Chou et al., 1996). Indeed, the OSM-6 protein shows some homology with the 40-kD mammalian protein NGD5, which was identified as an mRNA that is downregulated with prolonged exposure to an opioid receptor agonist and is thus involved in opioid receptor signaling (Wick et al., 1995; Collet et al., 1998). Both OSM-6 and NDG5 contain potential PxxP motifs that may modulate their interaction with other signaling molecules containing SH3 domains (Collet et al., 1998; Cole et al., 1998).

The transport of OSM-1::GFP, OSM-6::GFP, and KAP::GFP particles is likely to be physiologically relevant because they move very consistently at the same rate and share similar transport velocities, and because both the OSM-1::GFP and the OSM-6::GFP fusion proteins rescue the cilia defects of *osm-1* (Fig. 2) and *osm-6* (Collet et al., 1998) mutants, respectively. It is likely that the IFT rafts containing these proteins function to convey cargo by moving bidirectionally along the ciliary axoneme, picking up cargo in the cell body or at the transition zone, and delivering it to its site of activity or incorporation at the distal tip of the axoneme. The retrieval of kinesin-II and IFT raft particles to the transition zone or to the cell body by retrograde transport could then serve to regenerate the available pool of anterograde IFT motor and raft components.

What Drives the Anterograde Transport of OSM-1 and OSM-6 along Dendrites and Cilia?

The similar rates of anterograde transport of OSM-1::GFP, OSM-6::GFP, and KAP::GFP in both IFT transport along sensory cilia and dendritic transport along corresponding amphid neuronal dendrites, suggests, but does not prove, that these molecules share a common transport pathway from the cell bodies to the tip of the sensory cilium. Based solely on their similar transport rates and localization, it is plausible to suggest that OSM-1 and OSM-6 are transported by kinesin-II in both sensory cilia and sensory neuron dendrites. This is consistent with the suggestion that OSM-1 and OSM-6 polypeptides represent *C. elegans* homologues of proteins that are components of the IFT rafts that are transported by heteromeric FLA-10 kinesin in *Chlamydomonas* (Cole et al., 1998). In contrast, the diacetyl receptor, Odr-10, moves along dendrites at a faster rate (Orozco et al., 1999) and, thus, is thought to be transported by a kinesin-II–independent pathway.

In addition to heterotrimeric kinesin-II, *C. elegans* chemosensory neurons contain another heteromeric kinesin complex, Osm-3–kinesin. The Osm-3–kinesin motor does not appear to be responsible for the anterograde transport of IFT raft components as the OSM-6::GFP fusion protein localizes normally and demonstrates normal anterograde IFT and dendritic transport in the *osm-3* homozygous mutant background. To directly test the hypothesis that kinesin-II drives the anterograde transport of OSM-1 and OSM-6 will require a method for specifically inactivating this motor protein and assaying for a corresponding inhibition of the transport of OSM-1 and OSM-6 proteins. At the current time, the absence of a kinesin-II mutant makes this difficult and for this reason, we are currently undertaking a reverse genetic approach with the goal of identifying mutations in genes encoding kinesin-II subunits.

Evidence that CHE-3 Cytoplasmic Dynein Drives the Retrograde Transport of Kinesin-II and Its Cargo in Sensory Cilia, but Not in Dendrites

The availability of mutants in the *che-3* gene allowed us to assess the role of the cytoplasmic dynein CHE-3 in retrograde transport. Like anterograde transport, the retrograde IFT and dendritic transport of OSM-1, OSM-6, and KAP occur at similar rates, suggesting that they all may be transported retrogradely toward the transition zone (IFT) or toward the cell body (dendritic transport) by a common mechanism in wild-type worms. We have investigated if the minus end–directed microtubule motor, CHE-3 dynein, was responsible for the retrograde transport within sensory cilia and sensory neuron dendrites. We observed a specific inhibition of retrograde transport in cilia, but not in dendrites of *che-3* mutants, indicating a distinct subcellular transport role for the CHE-3 dynein in retrograde IFT.

CHE-3 is a divergent form of DHC that shares homology with DHC1b, the dynein isoform responsible for retrograde IFT transport in *Chlamydomonas* flagella (Pazour et al., 1998; 1999; Porter et al., 1999). The *C. elegans che-3* mutant has sensory cilia that lack the distal portions of their axoneme, but have normal looking axonemes lying adjacent to normal transition zones (Lewis and Hodgkin, 1977). Like *osm-1* and *osm-6*, *che-3* mutants show ectopic assembly of microtubules below the transition zones; but, in contrast to *osm-1* and *osm-6* which have normal diameter axonemes, *che-3* mutant cilia have enlarged, bulb-shaped tips filled with dark ground material (Lewis and Hodgkin, 1977). The dark material that accrues at the tips of *che-3* mutant sensory cilia is likely because of the accumulation of IFT rafts, representing proteins such as OSM-1, OSM-6, and kinesin-II. In support of this idea, we did observe an accumulation of OSM-6::GFP and KAP::GFP at the tips of sensory cilia and a loss of normal enrichment at the transition zone in *che-3* mutant worms, indicating defects in the retrograde transport of these proteins from the distal tip of the cilium back toward the transition zone. Although a mislocalization of OSM-6::GFP in *che-3* mutants has been seen before, it was reported as an accumulation in two large bilateral patches near the region of amphid neuron endings (Collet et al., 1998). By coupling high resolution confocal microscopy with the analysis of OSM-6::GFP and KAP::GFP transport in *che-3* mutants, we were able to directly visualize the anterograde IFT that leads to the accumulation of these proteins, to resolve the sites of accumulation at the distal tip of the cilia, and to document the absence of retrograde transport specifically in cilia

(but not the corresponding dendrites). Thus, CHE-3 cytoplasmic dynein is required for the retrograde IFT of kinesin-II and IFT raft particles along sensory cilia.

We are proposing that CHE-3 dynein functions as a motor that drives the retrograde transport of kinesin-II and IFT raft particles along axonemal microtubules in sensory cilia. However, we cannot formally exclude the possibility that the inhibition of retrograde IFT in *che-3* worms is an indirect, nonspecific consequence of the aberrant axonemes of *che-3* mutant cilia. Two key pieces of data seem to argue against this: (1) the ciliary defects would have to specifically affect retrograde transport since we see normal anterograde IFT along the shortened *che-3* axoneme; and (2) both anterograde and retrograde transport occur normally in the *osm-3* mutant background, which has similarly shortened axonemes. Although we cannot rule out the possibility that retrograde transport may require axonemal structures that are missing or aberrant in *che-3* mutants, such structures must be present in the *osm-3* mutant where retrograde transport occurs normally. Thus, the defective transport we see is specific for the retrograde direction, and is not a general consequence of ciliary structural deformity.

Although retrograde IFT is abolished in sensory cilia in the *che-3* mutant background, bidirectional transport occurs normally in the corresponding dendrite, indicating that CHE-3 dynein is not the retrograde motor for these molecules in sensory neuron dendrites. The *che-3 (e1124)* mutation is thought to be a null or severe loss-of-function allele (Wicks, S., C. deVries, H. Van Luenen, and R. Plasterk, manuscript submitted for publication; Grant, W., personal publication), so we cannot rule out the possibility that some residual CHE-3 activity may be sufficient to drive retrograde transport in dendrites but not in cilia. However, it is plausible that a different cytoplasmic dynein isoform or another minus end–directed motor protein may be responsible for the retrograde traffic of these and other proteins from the transition zone back to the cell body. Although abundant evidence exists implicating conventional kinesin, monomeric kinesins, and cytoplasmic dynein in bidirectional axonal transport (for reviews see Holzbaur and Vallee, 1994; Schnapp, 1997; Hirokawa, 1998), intradendritic transport has not been well characterized. However, since cytoplasmic dynein isoforms are thought to be responsible for fast retrograde axonal transport, it is plausible to propose they are also responsible for the retrograde transport of kinesin-II and associated cargo in *C. elegans* chemosensory dendrites.

There are at least two cytoplasmic DHC genes in *C. elegans*: one that is encoded by ORF T21E12.4 on genomic cosmid (GenBank accession number U80440) and more homologous to DHCs found in other organisms that are involved in various forms of intracellular transport (Lye et al., 1995); and CHE-3, which is encoded by the F18C12.1 ORF on cosmid F18C12 (GenBank accession number Z75536). The former was previously purified from whole worm extracts (Lye et al., 1987) and may be responsible for the retrograde dendritic transport of kinesin-II and cargo molecules. Alternatively, there are kinesin-related motors that have carboxy-terminal motor domains and are thought to move toward the minus ends of microtubules (Vale and Fletterick, 1997). In adult mouse neurons there is a carboxy-terminal motor, KifC2, which localizes to dendrites, axons, and cell bodies of neurons in the central and peripheral nervous systems (Hanlon et al., 1997; Saito et al., 1997). KifC2 may be involved in retrograde axonal transport (Hanlon et al., 1997) and/or the transport of multivesicular bodylike organelles in dendrites (Saito et al., 1997). The *C. elegans* genome sequencing project has identified at least six ORFs that may encode carboxy-terminal motor proteins and, therefore, potential retrograde transport motors, but a true homologue of KifC2 has not been described. However, it should be noted that the microtubule polarity in amphid and phasmid neuron dendrites has not yet been determined. A requirement for a minus end–directed motor would only be true if the microtubules in sensory dendrites are uniform, with plus ends distal to the cell body, similar to the uniform microtubule arrangement characteristic of vertebrate axons. If these dendritic microtubules are actually of mixed polarity, as seen in the dendrites of some vertebrate neurons (Heideman and McIntosh, 1980; Heideman et al., 1981; Baas et al., 1988; Burton, 1988), then in theory either plus or minus end motors could facilitate retrograde dendritic traffic.

The time-lapse fluorescence microscope–based assay described here allows the direct visualization of the in vivo transport of GFP-tagged motor and cargo molecules in both wild-type and mutant backgrounds, and enables us to assess the role of intradendritic and intraflagellar transport in chemosensory neuronal function and behavior in this simple animal. This approach has already revealed that the presumptive retrograde motor, CHE-3 dynein, participates in the retrograde intraflagellar transport of key ciliary components. Moreover, the transport pathway that we are studying appears to play a critical role in nervous system function as mutations in the *che-3*, *osm-1* and *osm-6* genes display severe defects in sensory cilia. Furthermore, because all known chemical attractants, repellents, and pheromones are sensed through ciliated receptors in *C. elegans* (Dusenberry, 1980; Perkins et al., 1986), these mutants are defective in many essential behaviors. The use of this transport assay in concert with the multiple mutants that exist in sensory ciliary structure and function (Starich et al., 1995) should allow a detailed elucidation of the role of motor and cargo molecules in the pathway of sensory ciliary assembly and function, and in other basic neuronal processes, many of which are likely to be conserved in higher organisms.

We thank Drs. Stephen Wicks, Ronald Plasterk (Netherlands Cancer Institute, Division Of Molecular Biology, Amsterdam, Netherlands), Warwick Grant (Flanders University, Adelaide, Australia), and Carl Johnson (Axys Pharmaceuticals, San Francisco, CA) for providing valuable and critical information on the cloning and nature of the *che-3* mutant. We also thank Drs. Jocelyn Shaw and Steven Stone (University of Minnesota, St. Paul, MN) for providing valuable information on the *osm-1* gene, Drs. Joel Rosenbaum (Yale University, New Haven, CT), Greg Pazour, George Witman (University of Massachusetts Medical School, Worcester, MA), and members of the Scholey lab for useful discussion and beneficial comments on this manuscript, Dr. Alan Coulson for providing genomic cosmid clones, Dr. Theresa Steinagle (CGC, University of Minnesota) for providing *C. elegans* mutant strains, and Heather Brown for technical advice.

This work was supported by the National Institutes of Health grant GM50718 to J.M. Scholey.

Submitted: 29 July 1999
Revised: 23 September 1999

Accepted: 23 September 1999

References

Baas, P.W., J.S. Deitch, M.M. Black, and G.A. Banker. 1988. Polarity orientation of microtubules in hippocampal neurons: uniformity in the axon and nonuniformity in the dendrite. *Proc. Natl. Acad. Sci. USA*. 85:8335–8339.

Bargmann, C.I., J.H. Thomas, and H.R. Horvitz. 1990. Chemosensory cell function in the behaviour and development of *C. elegans*. *Cold Spring Harbor Symp. Quant. Biol.* 55:529–538.

Bi, G.Q., R.L. Morris, G. Liao, J.M. Alderton, J.M. Scholey, and R.A. Steinhardt. 1997. Kinesin- and myosin-driven steps of vesicle recruitment for $Ca2^{+}$-regulated exocytosis. *J. Cell Biol.* 138:999–1008.

Brenner, S. 1974. The genetics of *Caenorhabditis elegans*. *Genetics.* 77:71–94.

Burton, P.R. 1988. Dendrites of mitral cell neurons contain microtubules of opposite polarity. *Brain Res.* 473:107–115.

Chalfie, M., and J. White. 1988. The nervous system. *In* The Nematode *Caenorhabditis elegans*. W.B. Wood, editor. Cold Spring Harbor Laboratory, Cold Spring Harbor, New York. 337–391.

Chou, J.H., E. Troemel, P. Sengupta, H. Colbert, L. Tong, D. Tobin, K. Roayaie, J. Crump, N. Dwyer, and C.I. Bargmann. 1996. Olfactory recognition and discrimination in *Caenorhabditis elegans*. *Cold Spring Harbor Symp. Quant. Biol.* 61:57–64.

Cole, D.G., S.W. Chinn, K.P. Wedaman, K. Hall, T. Vuong, and J.M. Scholey. 1993. Novel heterotrimeric kinesin-related protein purified from sea urchin eggs. *Nature.* 366:268–270.

Cole, D.G., D.R. Diener, A.L. Himelblau, P.L. Beech, J.C. Fuster, and J.L. Rosenbaum. 1998. *Chlamydomonas* kinesin-II–dependent intraflagellar transport (IFT): IFT particles contain proteins required for ciliary assembly in *Caenorhabditis elegans* sensory neurons. *J. Cell Biol.* 141:993–1008.

Collet, J., C.A. Spike, E.A. Lundquist, J.E. Shaw, and R.K. Herman. 1998. Analysis of *osm-6*, a gene that affects sensory cilium structure and sensory neuron function in *Caenorhabditis elegans*. *Genetics.* 148:187–200.

Criswell, P.S., L.E. Ostrowski, D.J. Asai. 1996. A novel cytoplasmic dynein heavy chain: expression of DHC1b in mammalian ciliated epithelial cells. *J. Cell Sci.* 109:1891–1898.

Culotti, J.G., and R.L. Russell. 1978. Osmotic avoidance defective mutants of the nematode *Caenorhabditis elegans*. *Genetics.* 90:243–256.

Dusenbery, D.B., R.E. Sheridan, and R.L. Russell. 1975. Chemotaxis-defective mutants of the nematode *Caenorhabditis elegans*. *Genetics.* 80:297–309.

Dusenbery, D.B. 1980. Responses of the nematode *C. elegans* to controlled chemical stimulation. *J. Comp. Physiol.* 136:327–331.

Dwyer, N.D. 1998. Odorant receptor localization to olfactory cilia is mediated by Odr-4 and Unc-101. Ph.D Thesis. University of California at San Francisco.

Fire, A. 1986. Integrative transformation of *Caenorhabditis elegans*. *EMBO (Eur. Mol. Biol. Organ.) J.* 5:2673–2680.

Gibbons, B.H., D.J. Asai, W.J. Tang, T.S. Hays, and I.R. Gibbons. 1994. Phylogeny and expression of axonemal and cytoplasmic dynein genes in sea urchins. *Mol. Biol. Cell.* 5:57–70.

Goldstein, L.S.B., and Z. Yang. 2000. Microtubule-based transport systems in neurons. *Annu. Rev. Neurosci.* In press.

Greene, J.H., and S. Henikoff. 1996. Kinesin Homepage. http://www.blocks.fhcrc.org./~kinesin/.

Hanlon, D.W., Z. Yang, and L.S. Goldstein. 1997. Characterization of KIFC2, a neuronal kinesin superfamily member in mouse. *Neuron.* 18:439–451.

Hedgecock, E.M., J.G. Culotti, J.N. Thomson, and L.A. Perkins. 1985. Axonal guidance mutants of *Caenorhabditis elegans* identified by filling sensory neurons with fluorescein dyes. *Dev. Biol.* 111:158–170.

Heidemann, S.R., and J.R. McIntosh. 1980. Visualization of the structural polarity of microtubules. *Nature.* 286:517–519.

Heidemann, S.R., J.M. Landers, and M.A. Hamborg. 1981. Polarity orientation of axonal microtubules. *J. Cell Biol.* 91:661–665.

Hirokawa, N. 1998. Kinesin and dynein superfamily proteins and the mechanism of organelle transport. *Science.* 279:519–526.

Holzbaur, E., and R.B. Vallee. 1994. Dyneins: molecular structure and cellular functions. *Annu. Rev. Cell Biol.* 10:339–372.

Johnson, K.A. 1995. Keeping the beat: form meets function in the *Chlamydomonas* flagellum. *Bioessays.* 17:847–854.

Johnson, K.A., and J.L. Rosenbaum. 1992. Polarity of flagellar assembly in *Chlamydomonas*. *J. Cell Biol.* 19:1605–1611.

Kozminski, K.G., K.A. Johnson, P. Forscher, and J.L. Rosenbaum. 1993. A motility in the eukaryotic flagellum unrelated to flagellar beating. *Proc. Natl. Acad. Sci. USA*. 90:5519–5523.

Kozminski, K.G., P.L. Beech, and J.L. Rosenbaum. 1995. The *Chlamydomonas* kinesin-like protein FLA10 is involved in motility associated with the flagellar membrane. *J. Cell Biol.* 131:1517–1527.

Kramer, J., R.P. French, E. Park, and J.J. Johnson. 1990. The *Caenorhabditis elegans rol-6* gene, which interacts with the *sqt-1* collagen gene to determine organismal morphology, encodes a collagen. *Mol. Cell. Biol.* 10:2081–2090.

Lewis, J.A., and J.A. Hodgkin. 1977. Specific neuroanatomical changes in chemosensory mutants of the nematode *Caenorhabditis elegans*. *J. Comp. Neurol.* 172:489–510.

Lye, R.J., M.E. Porter, J.M. Scholey, and J.R. McIntosh. 1987. Identification of a microtubule-based cytoplasmic motor in the nematode *C. elegans*. *Cell.* 51: 309–318.

Lye, R.J., R.K. Wilson, and R.H. Waterston. 1995. Genomic structure of a cytoplasmic dynein heavy chain gene from the nematode *Caenorhabditis elegans*. *Cell Motil. Cytoskeleton*. 32:26–36.

Marszalek, J.R., P. Ruiz-Lozano, E. Roberts, K.R. Chien, and L.S. Goldstein. 1999a. Situs inversus and embryonic ciliary morphogenesis defects in mouse mutants lacking the KIF3A subunit of kinesin-II. *Proc. Natl. Acad. Sci. USA*. 96:5043–5048.

Marszalek, J.R., J.A. Weiner, S.J. Farlow, J. Chun, and L.S. Goldstein. 1999b. Novel dendritic kinesin sorting identified by different process targeting. *J. Cell Biol.* 145:469–479.

Mello, C.C., J.M. Kramer, D. Stinchcomb, and V. Ambros. 1991. Efficient gene transfer in *C. elegans*: extrachromosomal maintenance and integration of transforming sequences. *EMBO (Eur. Mol. Biol. Organ.) J.* 10:3959–3970.

Morris, R.L., and J.M. Scholey. 1997. Heterotrimeric kinesin-II is required for the assembly of motile 9+2 ciliary axonemes in sea urchin embryos. *J. Cell Biol.* 138:1009–1022.

Nonaka, S., Y. Tanaka, Y. Okada, S. Takeda, A. Harada, Y. Kanai, M. Kido, and N. Hirokawa. 1998. Randomization of left-right asymmetry due to loss of nodal cilia generating leftward flow of extraembryonic fluid in mice lacking KIF3B motor protein. *Cell.* 95:829–837.

Orozco, J.T., K.P. Wedaman, D. Signor, H. Brown, L. Rose, and J.M. Scholey. 1999. Movement of motor and cargo along cilia. *Nature.* 398:674.

Pazour, G.J., C.G. Wilkerson, and G.B. Witman. 1998. A dynein light chain is essential for the retrograde particle movement of intraflagellar transport (IFT). *J. Cell Biol.* 141:979–992.

Pazour, G.J., B.L. Dickert, and G.B. Witman. 1999. The DHC1b (DHC2) isoform of cytoplasmic dynein is required for flagellar assembly. *J. Cell Biol.* 144:473–481.

Perkins, L.A., E.M. Hedgecock, J.N. Thomson, and J.G. Culotti. 1986. Mutant sensory cilia in the nematode *Caenorhabditis elegans*. *Dev. Biol.* 117:456–487.

Piperno, G., and K. Mead. 1997. Transport of a novel complex in the cytoplasmic matrix of *Chlamydomonas* flagella. *Proc. Natl. Acad. Sci. USA*. 94:4457–4462.

Piperno, G., E. Siuda, S. Henderson, M. Segil, H. Vaananen, and M. Sassaroli. 1998. Distinct mutants of retrograde intraflagellar transport (IFT) share similar morphological and molecular defects. *J. Cell Biol.* 143:1591–1601.

Porter, M.E., R. Bower, J.A. Knott, P. Byrd, and W. Dentler. 1999. Cytoplasmic dynein heavy chain 1b is required for flagellar assembly in *Chlamydomonas*. *Mol. Biol. Cell.* 10:693–712.

Riddle, D.L., M.M. Swanson, and P.S. Albert. 1981. Interacting genes in nematode dauer larva formation. *Nature.* 290:668–671.

Rosenbaum, J.L., D.G. Cole, and D.R. Diener. 1999. Intraflagellar transport: the eyes have it. *J. Cell Biol.* 144:385–388.

Saito, N., Y. Okada, Y. Noda, Y. Kinoshita, S. Kondo, and N. Hirokawa. 1997. KIFC2 is a novel neuron-specific C-terminal type kinesin superfamily motor for dendritic transport of multivesicular body-like organelles. *Neuron* 18: 425–438.

Sambrook, J., E.F. Fritsch, and T. Maniatis. 1989. Molecular Cloning: A Laboratory Manual. Second edition. Cold Spring Harbor Laboratory, Cole Spring Harbor, NY.

Schnapp, B.J. 1997. Retroactive motors. *Neuron.* 18:523–526.

Scholey, J.M. 1996. Kinesin-II, a membrane traffic motor in axons, axonemes, and spindles. *J. Cell Biol.* 133:1–4.

Shakir, M., T. Fukushige, H. Yasuda, J. Miwa, and S.S. Siddiqui. 1993. *C. elegans osm-3* gene mediating osmotic avoidance behaviour encodes a kinesin-like protein. *Neuroreport.* 4:891–894.

Signor, D., K.P. Wedaman, L.S. Rose, and J.M. Scholey. 1999. Two heteromeric kinesin complexes in chemosensory neurons and sensory cilia of *Caenorhabditis elegans*. *Mol. Biol. Cell* 10:345–360.

Starich, T.A., R.K. Herman, C.K. Kari, W.H. Yeh, W.S. Schackwitz, M. Schuyler, J. Collet, J. Thomas, and D. Riddle. 1995. Mutations affecting chemosensory neurons of *Caenorhabditis elegans*. *Genetics.* 139:171–188.

Tabish, M., Z.K. Siddiqui, K. Nishikawa, and S.S. Siddiqui. 1995. Exclusive expression of *C. elegans osm-3* kinesin gene in chemosensory neurons open to the external environment. *J. Mol. Biol.* 247:377–389.

Vale, R.D., and R. Fletterick. 1997. The design plan of kinesin motors. *Annu. Rev. Cell Dev. Biol.* 13:745–777.

Vaisberg, E.A., P.M. Grissom, and J.R. McIntosh. 1996. Mammalian cells express three distinct dynein heavy chains that are localized to different cytoplasmic organelles. *J. Cell Biol.* 133:831–842.

Walther, Z., M. Vashishtha, and J.L. Hall. 1994. The *Chlamydomonas* Fla10 gene encodes a novel kinesin homologous protein. *J. Cell Biol.* 126:175–188.

Ward, S., N. Thompson, J.G. White, and S. Brenner. 1975. Electron microscopic reconstruction of the anterior sensory anatomy of the nematode, *Caenorhabditis elegans*. *J. Comp. Neurol.* 160:313–317.

Wedaman, K.P., D.W. Meyer, D.J. Rashid, D.G. Cole, and J.M. Scholey. 1996. Sequence and submolecular localization of the 115-kD accessory subunit of the heterotrimeric kinesin-II ($KRP_{85/95}$) complex. *J. Cell Biol.* 132:371–380.

Wick, M.J., D.K. Ann, and H.H. Loh. 1995. Molecular cloning of a novel protein regulated by opioid treatment of NG108-15 cells. *Brain Res. Mol. Brain Res.* 32:171–175.